



Research Paper

Evaluation of the Cryogenic Effect on Friction Stir Processed AA7075/Si Matrix Nanocomposites

Navid Molla Ramezani¹, Behnam Davoodi^{1*}

¹School of Mechanical Engineering, Iran University of Science and Technology, Tehran, Iran

*Email of Corresponding Author: bdavoodi@iust.ac.ir

Received: November 13, 2023; Accepted: January 3, 2024

Abstract

Friction-stir processing is a green manufacturing process for surface composite fabrication and surface modification. To achieve this critical goal, the type of cooling and lubrication are of great importance. Therefore, in this paper, the cryogenic effects were investigated on friction-stir processing (FSP) tool wear and surface quality of an aluminum matrix nanocomposite. Silicon carbide (SiC) nanopowder was used as the reinforcing phase. The effects of cooling strategy and tool rotation speed on the tool wear, microhardness, surface roughness, and energy dispersive spectroscopy (EDS) analysis were studied. The cooling procedure was conducted under dry and cryogenic conditions. Additionally, the rotation speed was set at three levels, while other parameters were kept constant. The FSP tools were examined under a scanning electron microscope, and the wear mechanisms were investigated under different conditions. The results showed that tool wear, surface roughness, and microhardness were improved under cryogenic conditions compared to air conditions. Furthermore, in the presence of liquid nitrogen, the metal matrix composite did not exhibit any microstructural defects, such as micro-cracks. Energy dispersive spectroscopy analysis also demonstrated that SiC had better penetration into the base material under cryogenic conditions compared to dry conditions.

Keywords

Friction Stir Processing (FSP), Cryogenic, 7075 Aluminum Alloy, Tool Wear, Surface Quality

1. Introduction

Metal Matrix composites (MMC) due to their unique surface characteristics have so many usages in industries such as transportation, automobiles, medical, and power plants. It is noted that surface microhardness, corrosion resistance, and wear resistance are significant characteristics of surface metal matrix composites. This kind of surface composite, despite high surface hardness and strength, has the toughness of base metal. One of the most modern methods for making surface metal matrix composites is friction stir processing. This method was created because of the reinforcement and improvement of alloy characteristics. Friction stir processing (FSP) is a process that follows the principles of friction stir welding (solid-state joining method) [1-7]. Friction stir processing is one method in which a rotating tool penetrates the surface of the workpiece and by developing friction and stir, makes material flows, and distributes reinforcement particles [8-9]. This process is a

technique that improves the micro and macro properties of materials. When the process is worked out, the size of grains becomes small in the stir zone; consequently, due to the Hall–Petch relation, the mechanical resistance of the material is increased. Consequently, this method as a solid-state process, has been used instead of fusion methods, which causes microstructural deficiencies [10-12]. On the other hand, in friction stir processing, many input parameters have an essential role in microstructure improvement; they include machine parameters, tool parameters, and material properties. However, ambient factors, like the cooling process, have a significant role in this process. Many ambient and coolants can be used for friction stir bases operations such as air, warm and cold water, forced water, and water-ice mixture but liquid nitrogen with extreme cooling capacity due to its high latent heat of evaporation is an attractive coolant ambient for investigation [13].

Fratini et al. [14] in a study on friction stir welding of two similar AA7075-T6 alloys found that in specific rotation and traverse speed, cooling with water during the process leads to strength increase in the welding zone. The average mechanical resistance of welding joints fabricated in the water cooling ambient is a little bit higher than welding joints in normal conditions. Huang et al. [15], in an investigation on aluminum matrix composites made by friction stir processing submerged in water, used titanium particles as reinforcement powder. After completing three passes, titanium particles were distributed uniformly in the stir zone, and the grain size became 1 micrometer, improved by continuous dynamic recrystallization. Dong et al. [16] used submerged friction stir welding to join two similar Al7050 plates. In this experiment, warm and cold water were applied for cooling. They found that the highest tensile strength was achieved when warm water was used for cooling. Mothukuri et al. studied the effect of cooling with liquid nitrogen in friction stir welding of two dissimilar aluminum alloys (AA5080-AA6061) plates. The result showed that the weld line fabricated by square pin profile, the rotation speed of 900 rpm, the traverse speed of 31.5 mm/min, and a tilt angle of 2° led to the ultimate tensile strength of 180 MPa and the hardness of 82.8 HV. They also noted that in these parameters, the size of the grain in the stir zone reaches 4.2 micrometers. Sharma et al. [17] took out the overwhelming heat from the weld zone during friction stir welding of AA7039. They found that this action decreased the grain growth in that zone; the amount of microhardness by applying the cooling process using liquid nitrogen was higher than cooling using water. Also, microhardness in cooling conditions using air, had the lowest amount. Khodabakhshi et al. [18] studied producing Al-Mg composite by cryogenic friction stir processing. In this method, the workpiece is submerged in liquid nitrogen. The temperature of ambient in the cryogenics friction stir processing was about -196°C. This low temperature influences the material flow and makes it weak. Therefore, during the friction stir processing, with the weakness of material flow, a heterogeneous distribution of TiO₂ nanoparticles in the stir zone was seen. The homogeneous distribution of these particles was seen when a mixture of water and ice was used with a temperature of about 0°C. The aggregation of reinforcement particles in friction stir processing was due to the ambient conditions of this process.

Based on the literature, no experimental research has been reported on the main parameters of the tool wear, surface roughness, microhardness, and energy-dispersive X-ray spectroscopy (EDS) in the Al-SiC nanocomposite prepared by cooled friction stir processing. Therefore, in this research, the effects of different parameters are investigated by cooled friction stir welding processing on tool wear, roughness, microhardness, and the surface chemical composition of tools.

2. Materials and methods

In this investigation, silicon carbide nanopowder with a purity of 99%, between 45 to 65-nanometer dimensions, is used as an enhancer of mechanical base metal properties. The workpiece was an AA7075 plate in 200 mm×100 mm×10 mm, which has longitudinal grooves. The chemical compositions of the base material (Aluminum 7075) are shown in Table 1. The groove with 2mm width and 4mm depth was created in the workpiece by the milling process. Silicon carbide nanoparticles with a particular volume percent are placed and compressed in the groove. For capping the groove, a pinless tool with a 6-millimeter diameter from hot work tool steel (H13) was used. The next step for distributing the silicon carbide nanoparticles in a base metal context was friction stir processing. In this step, a tool including a pin and shoulder, was used. Tool chemical compositions, tool dimensions, and schematic of the experiment setup are shown in Table 2 and Figure 1, respectively.

Table 1. Chemical compositions (%) of the base material (Aluminum 7075)

Al	Si	Fe	Cu	Mn	Mg	Cr	Zn	Ti	V
Base	0.036	0.237	1.7	0.01	2.35	0.22	5.31	0.046	0.022

Table 2. Chemical compositions of the FSP tool

Fe	C	Si	Mn	S	Cr	Mo	Ni	Cu	Nb
Base	0.49%	1.1%	0.33%	0.01%	5.24%	0.9%	0.1%	0.069%	0.037%
W	Pb	As	Ce	Zn	Ti	V	Al	Co	
0.091%	0.01%	0.035%	0.011%	0.015%	0.012%	0.74%	0.044%	0.021%	

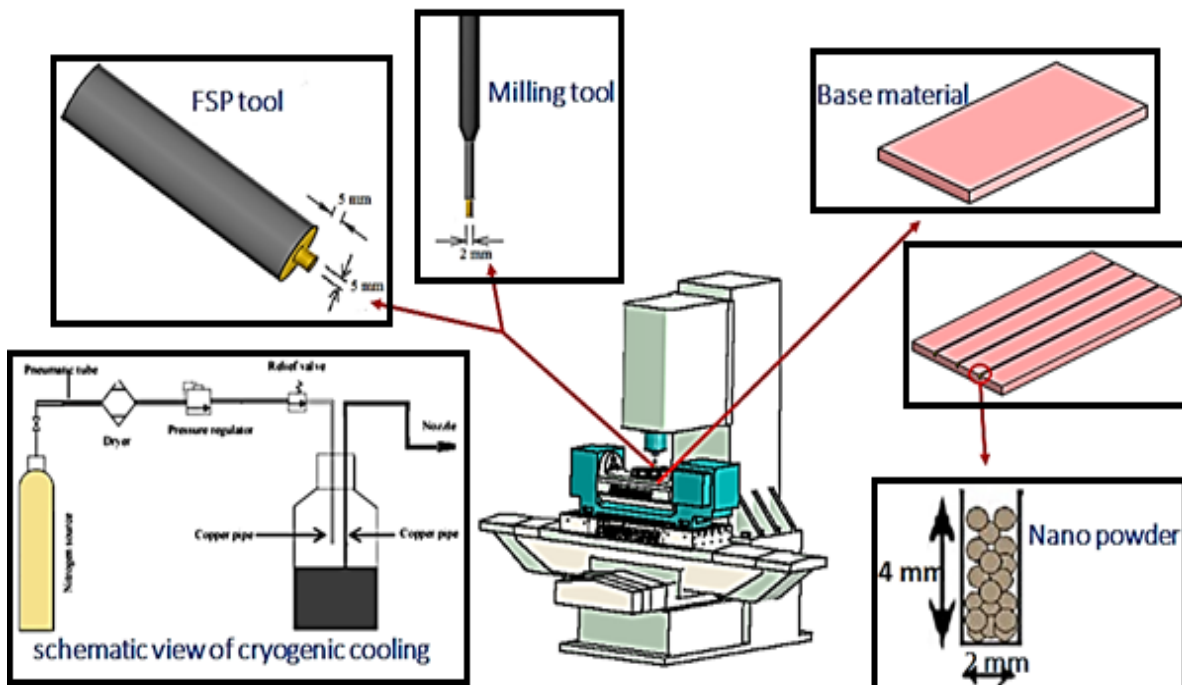


Figure. 1. Schematic of experiment setup

In this experiment, the rotation speed of 300, 900, and 1200 rpm were considered as input parameters. Also, the traverse speed of 30 mm/min was considered as a constant input parameter. Variable parameters with the levels are listed in Table 3. Another variable input parameter was a cooling strategy. Friction stir processing is carried out in the air and liquid nitrogen (cryogenic) ambient. Liquid nitrogen was used to decrease the ambient temperature of the stir zone. Liquid nitrogen was pumped to the contact zone of the friction stir processing tool and workpiece by a nozzle. In each of these conditions, three FSP passes were used for the reinforcement of base metal. After completing the process, for microstructure analysis, the samples were cut in cross-sections, and then cold mounted. For microhardness assessment in each sample, three points of stir zone were measured, and the average of these three amounts was recorded as a final microhardness amount. The accuracy of the digital microhardness taster was 1 Vicker. Also, by applying an optical microscope and SEM, tool wear was evaluated.

Table 3. Input parameters and levels

Levels	Parameters		
Rotation speed (rpm)	300	900	1200
Cooling strategy	Cryogenics		Air
Traverse speed (mm/min)	30		
Pass number	3		

3. Results and discussion

3.1 Tool wear

Tool wear is a significant challenge in many industries. The tool wear reduction has a substantial effect on economic aspects and product quality. The tool wear in some processes like machining and friction stir welding and processing is high and very important, and many kinds of research must be done for the reduction of tool wear [19-21]. In this case, tool wear is mainly caused by the contact of the tool pin and the harsh SiC nanoparticles and the residual by the contact and adhesion of aluminum base metal, and these two reasons are caused by the complex material flow. The study of tool wear in friction stir welding and processing is insufficient. The tool wear in FSP is too complicated, but some hypotheses can be considered for the evaluation of tool wear in FSP. Tool wear happens due to the interaction of the rotating pin with the base material and reinforcing particles. Ceramic reinforcing particles like SiC because of their sharpness and hardness can wear any metal. Different parameters like rotational speed, tool traverse speed, pass number, materials, and even cooling conditions influence tool wear in FSP [22]. Ramezani et al. [23-24] investigated that rotational tool speed has a significant effect on tool wear and wrap and the tool wear decreases with increasing the tool rotation speed. This is because of the temperature effect on material softening. Whatever rotational speed increases, the temperature and frictional heat input increase and make the material softer. The decrease in tool hardness is less than the base metal during frictional heating [3]. So, the relative hardness between the tool and workpiece increases, and tool wear can be less. Much of the tool wear is because of the interaction of abrasive ceramic SiC Nanoparticles. The nano-size reinforcing particle has an extensive interface with the tool and can wear every non-smooth geometry like threads. The material flow is parallel with the tool pin and can circulate the tool pin and SiC

Nanoparticles remove all the threads. If there was a chance to control material flow while it supports insufficient flow but is not unnecessary; the tool wear can be genuinely better.

Fernandez and Murr [25] examined that after a defined working length, the tool pin is smoother. The geometry of the tool pin is like an hourglass that is named the self-optimized shape. From this stage, tool wear decreases to an ignorable value. So, with this discussion, we must control the material flow, heat input, and peak temperature, and make the tool smoother and self-optimized shape as soon as possible in processing to decrease the tool wear. That is mentioned that cooling is a crucial factor for tool wear. Cryogenic cooling conditions prepare a very chilled temperature of about -196 degrees Celsius in the tank and subzero temperatures when getting free in the atmosphere (about -30 degrees Celsius). The liquid nitrogen cooling rate is higher than conventional cooling liquids, and it is an excellent property for our goal. The peak temperature and the cooling rate are critical factors in the tool wear issue liquid nitrogen can influence both factors [26]. The low peak temperature causes insufficient material flow, and the softness of the base material is low, simultaneously, the distribution and dispersion of Nanoparticles are inadequate because of poor material flow [18]. Likewise, the high peak temperature is terrible due to its effect on tool hardness dropping. It can be understood that the peak temperature has an optimum value to keep the relative hardness between the tool and workpiece at the maximum value for minimum tool wear. In high rotational speed (about 1500 rpm and higher), the frictional heat input and the peak temperature are high causing more base material softness and hardness dropping of the tool; if we can control the temperature peak simultaneously that the material softness is sufficient, we can achieve the optimum situation of minimum tool wear. Cryogenic cooling with a high cooling rate of liquid nitrogen can prepare for this situation. Zhang et al. [26] studied the FSW of high-nitrogen stainless steel in two different situations, forced water cooling, and ambient air cooling. They found that temperature curves could explain the tool wear in the process. They found that the tool wear can be less with highly efficient water cooling due to tool hardness retaining. The material flow in the different cooling conditions is different. As Prado et al. [27] mentioned, the self-optimized shape tool is a geometry in that the keen side of the tool is worn or hidden, and the material flow passes the tool surface very smoothly. The key to the investigation of tool wear is the self-optimized shape formation as a function of process parameters, and the sooner formation can provide less tool wear. Figure 3a shows the first tool before FSP, Figure 3b shows the tool pin profile at air cooling condition, and Figure 3c shows the pin profile at the cryogenic cooling condition with the same process parameters as rotational speed, tool traverse speed, and the passes number (three passes). It can be understood that tool wear in the air cooling more than the cryogenic cooling due to lower wear of threads in the cryogenic condition that it is clear for lower threads cut section and more threads spacing. The pin profile in the air-cooling condition is more like an hourglass shape Murr noted that in air cooling condition. As can be seen, that self-optimized shape is formed when the shape and the threads are not more recognizable like in Figure 3b, but there is no reason we have not approach to self-optimized shape in a cryogenic ambient. The two different worn tool profiles are self-optimized bur; they are different due to the difference of their material regime and self-optimized tool pin profile in the cryogenic condition achieved sooner. We want to discuss the following reasons for this fact. The distribution of Nanoparticles is highly dependent on the processing environment and cooling conditions. Poor material flow with low heat input caused by low rotational speed or more cooling, makes the Nanoparticle agglomerated. It can be the reason for more tool wear at a lower

rotational speed due to the role of SiC particles in wear. The hardness retaining of the base material in low rotational speed in cryogenic FSP can be another reason for more tool wear due to the base material's role in the wear. However, it seems to be not adequate in comparison to the other Events. G.J. Fernandez et al. [25] note that the material flow in friction stir welding has two different mechanisms. The whirling flow around the tool pin axis extrudes material from behind the tool to its front and makes severe strain rate, and another is another whirling flow of material around an axis that is perpendicular to the tool pin axis. The vertical flow of the transverse cut section has a significant effect on the homogeneity of distributed nanoparticles and complete material flow for the reinforcing purpose. R. Nandan et al. [28] note the radius of the low-viscosity material (in this case mild steel) enhanced with the depth of the workpiece, and the material flow is more in the vicinity of the pin tip. So, the velocity is increased with an increase in depth, and the velocity has a direct relation with viscosity. Finally, it turns out that the velocity and total material flow can decrease with viscosity decreasing. The temperature drop can cause an enhancement in viscosity and can decrease the velocity and the material flow. Liquid nitrogen, with its extreme cooling capacity, can decrease the peak temperature. The duration of the peak temperature, viscosity, and material flow, velocity of the flown material, and the volume of the flown material can be dramatically reduced. Due to the direction of active cooling in the depth of the workpiece via liquid nitrogen, the vertical material flow can be suppressed, and reduced material flow, especially in the vertical direction, dominates. Since the reinforcement particle cannot approach the surface and move down again and its movement turns to limited height with high viscosity and low velocity, the SiC particles have little chance to wear the body of the threads. This fact is caused by less SiC distribution and more agglomeration in the depth of the workpiece [18, 29, 30]. Due to poor vertical material flow during liquid nitrogen cooling, the threads can be filled sooner with aluminum. The aluminum can stick on the thread's tool surface via a weak cooling effect in this location and rises to approach the thread surface. Due to the less softening of the base material and poor vertical material flow, not only the stuck material on the threads do not pull out the threads, but the material segregated more brittle to give the material around the tool pin the freedom to quickly vortex. This fact can be seen in Figure 3c to compare Figure 3b. in the highest magnitude SEM picture, the cryogenic tool surface has more brittle segregation compared to the smooth surface of the air-cooled tool due to the light white boundaries that show the height difference and more brittle segregation. It can be concluded that the whole material flow in both volumetric and velocity points of view decreased, and the vertical material flow was suppressed by cooling and viscosity increase. Due to all the above discussion, the reduced material flow caused by cryogenic high-capacity cooling can reduce the tool wear via faster tool self-optimized shape formation caused by different material regimes that occur in this case. Figure 2 shows the tool wear as a function of rotational tool speed and ambient situation. This figure indicates that tool wear can be reduced via the cryogenic cooling condition and the increase of rotational tool speed. As the tool rotational speed increases, the heat input increases, and this fact has two significant effects; firstly; more heat input can support complete material flow for filling the root of the threads, and with the cryogenic cooling situation it can be suppressed immediately after threads filling and this fact can help the tool to provide its self-optimized shape as soon as possible. Secondly, more heat input can reduce viscosity, and this fact has a non-committal effect on tool wear. In the first point of view, the viscosity reduction can cause more volume for the flown material, and in another point of view, its viscosity reduction

can decrease the rubbing force. It can be concluded that the second effect can have an optimum, but its effect is so less than the first effect [23-31]. The distribution of Nanoparticles is highly dependent on the processing environment and cooling conditions. A poor material flow during cryogenic FSP with low rotational speed makes the Nanoparticle agglomerated, and it can be the reason for more tool wear at lower rotational speed due to the role of SiC particles in wear. The hardness retaining of the base material in low rotational speed in cryogenic FSP can be another reason for more tool wear due to the base material's role in the wear, but it seems to be not effective in comparison to the other Events. Figure 3a shows the first tool before FSP, Figure 3b shows the tool pin profile at air cooling conditions, and Figure 3c shows the pin profile at the cryogenic cooling condition with the same process parameters as rotational speed, tool traverse speed, and the passes number. It can be understood that tool wear in the air cooling more than the cryogenic cooling due to lower wear of threads in the cryogenic condition that it is clear for lower threads cut section and more threads spacing. The pin profile in the air-cooling condition is more like an hourglass shape that v noted that in air cooling condition. As can be seen, a self-optimized shape is formed when the shape is smothered, and the threads are not more recognizable like Fig 3b, but there is no reason we have not approached a self-optimized shape in a cryogenic ambient. The two different worn tool profiles are self-optimized bur; they are different due to the difference of their material regime and self-optimized tool pin profile in the cryogenic condition achieved sooner. The main material flow that has been described by G.J. Fernandez et al. in the last paragraphs existed in the air-cooling condition, but the amount of the material flow and the exact material regime are different from the cryogenic cooling condition. In the air-cooling condition, the amount of the flown material is more due to the higher viscosity domain due to lower cooling and higher peak temperature. The main practical difference between cryogenic and air-cooling conditions is the vertical material flow that is suppressed at low peak temperature and instant viscosity enhancement due to the high cooling capacity of liquid nitrogen in the cryogenic effect and can preserve the harsh nanoparticles below the tooltip. The complete vertical material flow in the air-cooling condition makes the more velocity and chance for the abrasive SiC nanoparticle to contact with the tool pin, and the tool wear with these two reasons can be more significant in the air-cooling condition case. The filling of tool pin threads can be longer due to the more material softening in the air-cooling condition, but in the cryogenic condition after little wear of threads in higher rotational speed, the base material can be filling the threads and like that, no threads exist. The self-optimized shape was achieved sooner with lower threads wearing in cryogenic cooling conditions due to all the discussion.

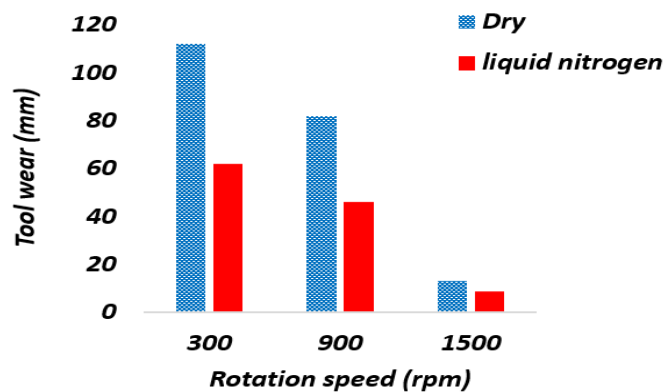


Figure 2. Effect of Rotation speed on tool wear

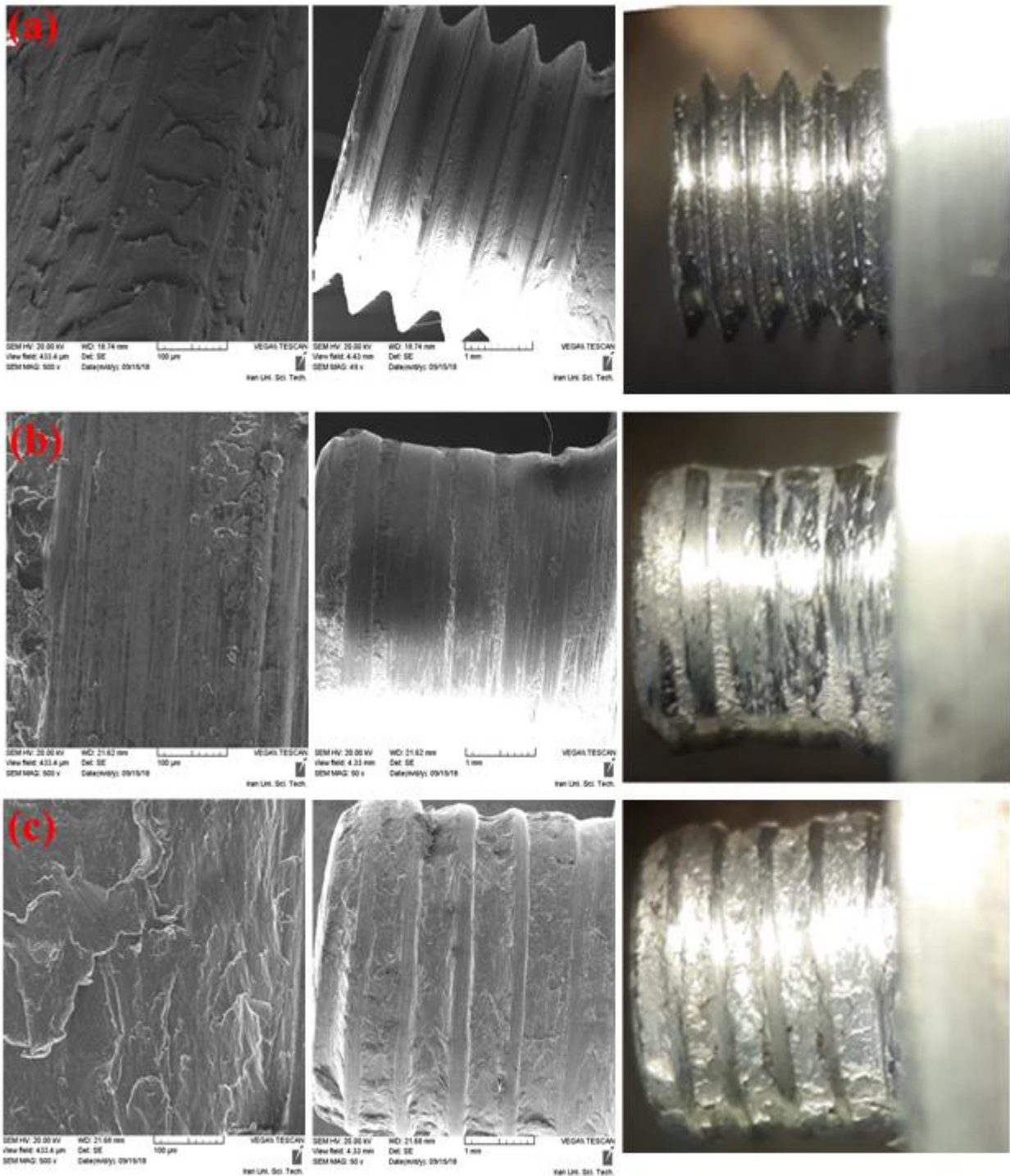


Figure 3. Tool wear in the rotation speed of 1500 rpm, traverse speed of 30 mm/min, and three passes with SEM and optical microscope a) primary tool b) air condition c) cryogenics condition

3.2 Microhardness

It is necessary to describe the microstructure analysis to a better justification for microhardness. The heat-affected zone (HAZ) is the most impoverished region in each FSP sample. M. Sarkari Khorrami et al. [13] observed that the Nano-composite fabricated via FSP with SIC particles under ambient

temperature has a quiet large grain structure with random texture in vast HAZ region due to the occurrence of static grain racialization and grain growth because of high peak temperature and spend the most time in this temperature. Under the cryogenic condition, bimodal grain size distribution in HAZ was observed, including the elongated grains with interior subgrains. More passes number causes more random texture in HAZ. The microhardness of the HAZ under cryogenic conditions was improved due to stopping the grain growth and reducing the time spent at the peak temperature due to a higher cooling rate, which makes the HAZ thinner. When the FSP occurs under the cryogenic condition, the grain formed in the stir zone will be smaller due to the higher cooling rate of liquid nitrogen in the stir zone (SZ) [32]. For this high cooling rate of cryogenic condition; the grain formation mechanism changes to discontinuous dynamic recrystallization (DDRX).

The research shows that the SZ texture in the ambient and cryogenic conditions is almost similar (simple shear texture). In both conditions, the grain formation mechanism is dynamic recrystallization, but in the cryogenic condition, it shows less dynamic behavior due to the ultra-cooling rate. The SIC Nanoparticles play a pinning role on grain boundaries to form better grain. When the SIC particle pins the grain boundaries, it can create a problematic situation informing the grain orientation along with the shear stress of the rotating tool. The Orowan strengthening mechanism plays an essential role in the stir zone and makes the dislocation turn around not-sharable SIC particles [13]. The main difference between air-cooled and other cooling conditions is the peak temperature and high-temperature exposure duration [26]. The highest hardness of the nugget zone (NZ) or stir zone (SZ) is mainly attributed to the ultra-fine grain structure that is achieved by controlling the peak temperature and duration time at this condition [16]. Under the cryogenic condition, high angle, ultra-fine grains, and cellular structures with sizes commonly smaller than $1\mu\text{m}$ are attained that show significant improvement in strength and hardness. The submicron grain structure that is formed under the effect of SPD and high cooling rate can provide an ultra-fine grain (UFG) structure with a unique combination of strength, hardness, and superplastic behavior with improvement in ductility.

H.J. Zhang et al. [33] found that the grain structure and the mechanical properties were sensitive to processing parameters, especially the peak temperature and the rotational speed. The high amount of sub-grains forms via dislocation intersection and accumulation during SPD under controlled cooling conditions. The pinning effect of the SIC reinforcing particles improves the thermal stability of the UFG sample. With the above discussion, it can be understood that with the cooling rate for controlling peak temperature and duration time at this temperature, the mechanical properties of SZ and HAZ can be improved due to the discontinuous dynamic recrystallization (DDRX) grain formation mechanism for UFG structure. For this opinion, the grain growth must be stopped, and the grain boundaries must be pinned. In UFG materials, the length of dislocation pileup is limited, and higher applied stress is required to promote slip transmission across grain boundaries.

Another factor that may influence the microhardness of the FSP product from Aluminum 7xxx is the dissolution of the hard precipices during the FSP. The aluminum 7xxx series is the heat-treatable one and because of Mg_2Zn deposition has a η hard phase [34]. The dissolution of deposition in treatable heat aluminum has a peak temperature with a period for diffusion. The kinetics of precipices coarsening are a maximum of 350°C for 7xxx all series, and the rate of formation of the non-strengthening η phase is at the peak near this temperature [35]. Many researchers have studied the

precipices after the processing and concluded that grain growth dissolution and coarsening during FSP occur very quickly due to the slow cooling rate and showing inferior properties [36]. Under the cooling condition, the NZ exhibits hardness which is equivalent to a T6 temper, and the base metal (BM) exhibits T7 (slightly over-aged) hardness. Due to equation 1, a (Hall-Petch strengthening), the hardness improvement can be justified.

$$\sigma_y = \sigma_0 + k/\sqrt{d} \quad (1)$$

The σ_0 is the frictional stress (≈ 20 Mpa), the k is the Hall-Petch constant (≈ 0.12 Mpa/(m)^{1/2}) and the d is of average grain size. This equation shows that the strength increased with grain size decreasing. In the cryogenic condition, the grain size dramatically decreased, and the hardness and strength increased in all regions, especially in SZ.

Figure 4 shows the microhardness value as a function of rotational tool speed and the cooling condition, while other process parameters are constant (3 passes number). The results show that the hardness can be improved by increasing rotational speed and cryogenic cooling conditions. The rotational speed can cause more strain rate and can reduce the grain size dramatically due to the Hall-Petch equation and all the below equations. The microhardness can be improved by the cryogenic cooling condition via discontinuous dynamic recrystallization (DDRX). DDRX suppresses the grain growth after nucleation and can suppress even more nucleation and can in more stable regions and provide a combination of the small, nucleated grain and some work-hardened areas with high dislocation density that can provide more hardness. Also, the complete material flow can occur at a higher rotational speed, and the density of the hard nanoparticles increases on the surface and can provide more hardness. A more comprehensive discussion has been presented below. Forasmuch as the FSP is a thermos-mechanical process; in addition to heat input and the peak temperature, the strain rate is essential (Equation 2 is an experimental relation).

$$\dot{\varepsilon} = \frac{k\pi\omega r_e}{l_e} \quad (2)$$

Where the $\dot{\varepsilon}$'s strain rate; the k is a constant with a nominal value of 1; the ω is the angular speed attributed to the rotational speed; the r_e and l_e is the effective radius and adequate depth of the dynamically recrystallized zone. The results show that the r_e and l_e reduce in higher cooling rate and $\dot{\varepsilon}$ a little less than air cooling condition obtained, but it is ignorable. It can be seen that $\dot{\varepsilon}$ increases with tool rotational speed increasing. The $\dot{\varepsilon}$ and the peak temperature can be controlled to achieve the best mechanical properties. The Zener-Holloman parameter shown in Equitation 3 contains the compound effect of both $\dot{\varepsilon}$ and the peak temperature.

$$Z = \dot{\varepsilon} \cdot e^{\left(\frac{Q}{RT}\right)} \quad (3)$$

Where the Z is Zener-Holloman parameter; $\dot{\varepsilon}$ is strain rate; Q is activation energy (142 J/mol.K; R is the Global constant of gases (8.314 J/mol.K) and T is deformation temperature. The grain size can be found. Using equation 4; A and B are constant.

$$\ln^d = A - B \ln^z \quad (4)$$

As can be seen with increasing in the Z parameter; the d (grain size) changes to a lower value and decreases. The Z parameter increases in cryogenic conditions, and the grain size reduces according

to Equitation 4. Since Z is a function of $\dot{\epsilon}$ and the temperature, the temperature is lower in cryogenic conditions, so the Z in the cryogenic condition has a more significant value and leads to a smaller grain size. So, the grain size in the cryogenic condition is smaller than ambient air cooling due to a more significant Z value because of lower peak temperature and suppression of the grain growth that is affected by the higher cooling rate of liquid nitrogen.

Figure 4 shows the effect of cryogenic cooling on microhardness. As can be seen, the result shows the improvement in cryogenic high cooling rate. The hardness improvement at 1500 RPM is less than 600 RPM because the process temperature at 1500 RPM is near the dissolution temperature, some hard phases disappear, and some non-strengthening phases can be formed. The dissolution of strengthening phases did not occur at 600 RPM. Due to equation 2, the $\dot{\epsilon}$ has a higher value because of higher tool rotational speed. The grain size in the higher rotational speed is smaller due to an increase in Z parameter value, so the microhardness can be more in higher rotational speed that concluded from the Hall-Petch equation. The cryogenic condition with excellent tool rotational speed in heat-treatable 7xxx aluminum can improve the hardness and other mechanical properties due to the higher cooling rate of liquid nitrogen and forming ultra-fine grain (UFG) while keeping the hard precipitates of the base metal.

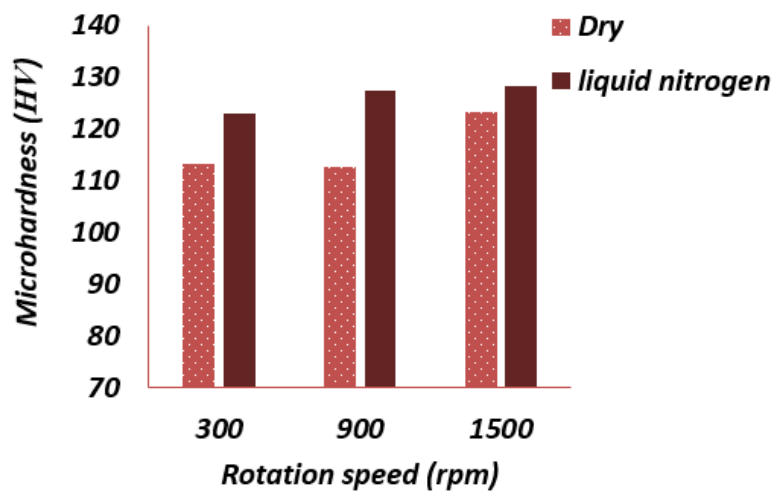


Figure 4. Effect of Rotation speed on microhardness

3.3 Surface roughness

Surface roughness is generated from two reasons in each process: the ideal or geometric finish and the natural finish. Ideal or geometric finish results from the kinematic motion of the tool and the interaction of the tool and workpiece surfaces and hardness. The natural finish can result from vibration and tool interface wear in our case [30, 37-39]. Figure 5 shows the relation between surface roughness and tool rotational speed; as can be seen, the surface roughness dramatically decreases with the tool rotational speed increasing. One of the most critical factors in workpiece surface roughness is the tool surface roughness, especially in the shoulder. The tool shoulder surface slides on the workpiece surface and scratches the surface of the workpiece.

As mentioned, the higher rotational speed causes more heat input, and more heat input makes the base material soft and makes the surface smoother, and the particle distribution more uniform [40-43]. As a result of more substantial severe plastic deformation (SPD) in higher tool rotational speed,

the smaller grain can be formed due to a higher strain rate. So, the smaller grain provides lower surface roughness and a better surface finish. Whatever the base material is soft, the scratch effect is fewer, and the effect of tool surface roughness is negligible. As expected, the higher rotational speed causes lower workpiece surface roughness because of higher heat input. In another view, the higher rotational speed cracks scratch better. Because of the higher value of speed, the peak of the tool shoulder roughness has more chance to crack the scratch of the workpiece surface and make it smoother. Typical cooling cutting fluid applied conventionally cannot reduce the interface temperature of the tool and workpiece effectively because of its unsuccessful penetration into the working region, especially at the high processing velocity.

Nevertheless, as Figure 5 shows, the surface roughness can be decreased in cryogenic high cooling rate conditions. During FSP, the surface adhesive base material can stick on the tool's shoulder surface and increase the surface roughness. However, in cryogenic conditions, it can be less due to a higher cooling rate. The better grain formation in cryogenic conditions provides a higher hardness value that the workpiece surface can resist scratching, and the surface finish can improve. It has been known that the surface roughness can increase with the feed rate increase and decrease with the cutting speed increase [44]. The comparison of surface roughness in cryogenic conditions and ambient air conditions is mainly attributed to tool wear. Whatever the tool wear is high, the tool cannot provide the heat input that the process needs to be more plastic for completion of the process. As mentioned, tool wear decreases in cryogenic conditions. The cryogenic condition reduces the tool wear, especially in the tool shoulder, keeps the tool hardness very well, and can improve tool life substantially. The surface roughness can be determined with the material removal rate. If many flashes are observed, it can be concluded that the surface roughness is inferior. The rough surface usually has a higher friction coefficient and tool wear. The characterization of tool wear was discussed in brief in the previous part of this article.

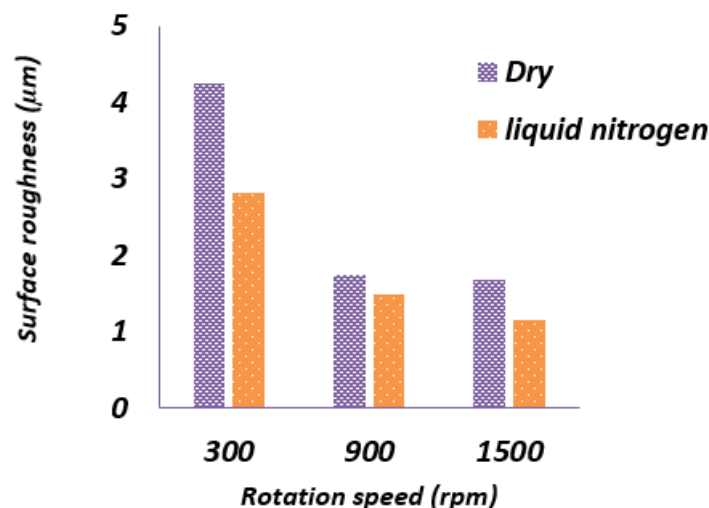


Figure 5. Effect of Rotation speed on surface roughness (Ra)

3.4 EDS analysis

EDS or energy-dispersive X-ray spectroscopy (EDS) analysis was done to assess the weight percent composition of the workpiece in different conditions of the friction stir process. Therefore, the EDS analysis was performed in all tests of this research for metal matrix composites and tools.

The result and analysis revealed that the SiC has suitable penetration in base material due to the existence of liquid nitrogen coolant than in dry condition (Figure 6). Also, in the cryogenic condition, the aluminum element was higher in the surface of the material than in dry condition. In other words, in dry conditions, nano powder cannot deeply penetrate the base metal. Instead, Figure 7 shows the chemical elements of the FSP tool.

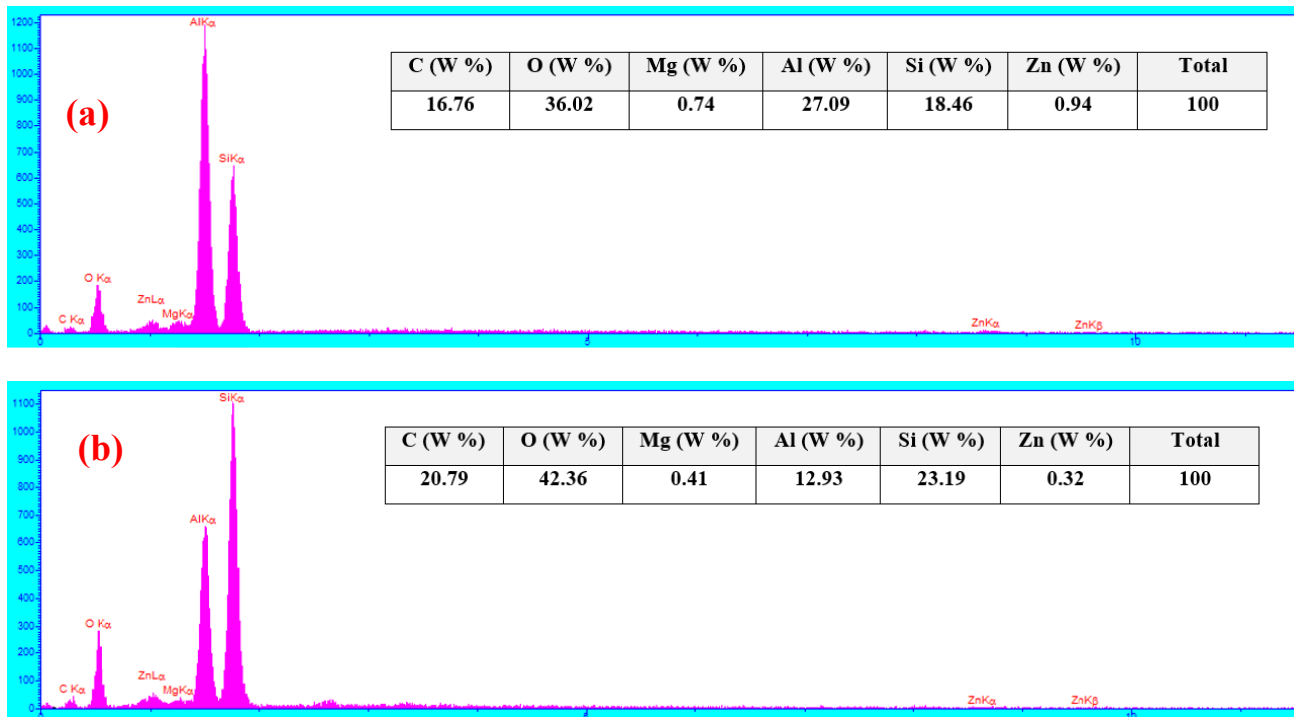


Figure 6. EDS analysis of FSPed in rotation speed 1500 rpm, traverse speed 30 mm/min, and with three passes a) cryogenics condition, b) air condition

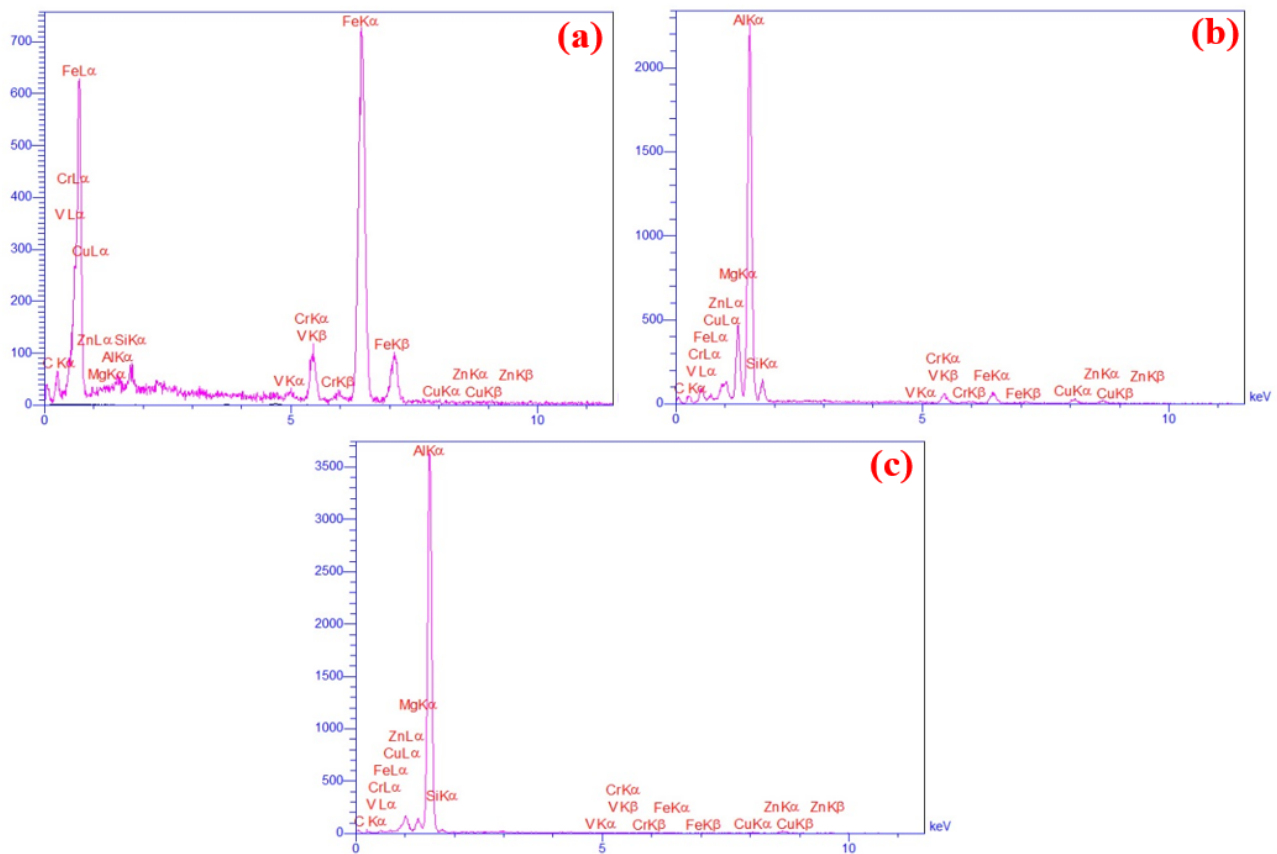


Figure 7. EDS analysis of tools in (a) primary tool, (b) air condition, (c) cryogenics condition

4. Conclusion

In this research, tests were done randomly to avoid errors in experiments. The main parameters were rotational speed and cooling conditions. Rotational speed and cooling conditions were set in 3 levels and two levels respectively to investigate tool wear, surface roughness, microhardness, and EDS analysis. Each experiment was done at the specimen length. The achieved conclusions are summarized here:

The tool wear decreases with a rotational speed increase. Also, the surface quality increased by rotational speed is increasing. This trend is at high temperatures due to proper plastic deformation, which is owing to lower forces and friction. Moreover, tool wear, surface roughness, and microhardness were improved in cryogenic conditions than in air conditions. Furthermore, with the existence of liquid nitrogen, nano powder penetration was suitable, and the metal matrix composite did not have any microstructure defect such as micro crack. The energy-dispersive X-ray spectroscopy (EDS) analysis was done in all experiments. The results revealed that the weight percentage of the tool elements and base metal elements changed after the friction stir processing. SiC has suitable penetration in base material due to the existence of liquid nitrogen than the dry condition.

5. Acknowledgment

The authors acknowledge the provision of research facilities used in this work by the research board of the Iran University of Science and Technology (IUST).

6. References

- [1] Padhy, G., C. Wu, and S. Gao. 2018. Friction stir based welding and processing technologies-processes, parameters, microstructures and applications: A review. *Journal of Materials Science & Technology*. 34(1): 1-38. doi: 10.1016/j.jmst.2017.11.029.
- [2] Adiga, K., Herbert, M.A., Rao, S.S. and Shettigar, A. 2022. Applications of reinforcement particles in the fabrication of aluminium metal matrix composites by friction stir processing-A review. *Manufacturing Review*. 9:26. doi: 10.1051/mfreview/2022025.
- [3] Mishra, R.S. and Z. Ma. 2005. Friction stir welding and processing. *Materials science and engineering: R: reports*. 50(1-2): 1-78. doi: 10.1016/j.mser.2005.07.001.
- [4] Mishra, R.S., Z. Ma, and I. Charit. 2003. Friction stir processing: a novel technique for fabrication of surface composite. *Materials Science and Engineering: A*. 341(1-2): 307-310. doi: 10.1016/S0921-5093(02)00199-5.
- [5] Hajideh, M.R., M. Farahani, and N.M. Ramezani. 2018. Reinforced dissimilar friction stir weld of polypropylene to acrylonitrile butadiene styrene with copper nanopowder. *Journal of Manufacturing Processes*. 32: 445-454. doi: 10.1016/j.jmapro.2018.03.010.
- [6] Hajideh, M. R., Farahani, M., Alavi, S. A. D., & Ramezani, N. 2017. Investigation on the effects of tool geometry on the microstructure and the mechanical properties of dissimilar friction stir welded polyethylene and polypropylene sheets. *Journal of Manufacturing Processes*. 26:269-279. doi: 10.1016/j.jmapro.2017.02.018.
- [7] Hajideh, M. R., Shapurgan, O., Ramzani, N. M. and Nejad, E. H. 2017. Friction stir welding of dissimilar poly methyl methacrylate and polycarbonate sheets. *Journal of Modern Processes in Manufacturing and Production*. 6(4): 35-46. doi: 10.1001/1.27170314.2017.6.4.3.0.
- [8] Abushanab, W. S., Moustafa, E. B., Goda, E. S., Ghandourah, E., Taha, M. A. and Mosleh, A. O. 2023. Influence of Vanadium and Niobium Carbide Particles on the Mechanical, Microstructural, and Physical Properties of AA6061 Aluminum-Based Mono-and Hybrid Composite Using FSP. *Coatings*. 13(1): 142. doi: 10.3390/coatings13010142.
- [9] Kumar, T. S., Thankachan, T., Shalini, S., Čep, R. and Kalita, K. 2023. Microstructure, hardness and wear behavior of ZrC particle reinforced AZ31 surface composites synthesized via friction stir processing. *Scientific Reports*. 13(1): 20089. doi: 10.1038/s41598-023-47381-5.
- [10] Diaz, O. G., Luna, G. G., Liao, Z. and Axinte, D. 2019. The new challenges of machining Ceramic Matrix Composites (CMCs): Review of surface integrity. *International Journal of Machine Tools and Manufacture*. 139: 24-36. doi: 10.1016/j.ijmactools.2019.01.003.
- [11] Keshavarz, H. and A.H. Kokabi. 2023. Influence of pass number on microstructure, mechanical, and tribological properties of cold-rolled Al1050 during friction stir processing. *Journal of Materials Research and Technology*. 27: p. 932-943. doi: 10.1016/j.jmrt.2023.10.032.
- [12] Wu, B., Ibrahim, M. Z., Raja, S., Yusof, F., Muhamad, M. R. B., Huang, R. and Kamangar, S. 2022. The influence of reinforcement particles friction stir processing on microstructure, mechanical properties, tribological and corrosion behaviors: A review. *Journal of Materials Research and Technology*. 20:1940-1975. doi: 10.1016/j.jmrt.2022.07.172.
- [13] Khorrami, M. S., Kazeminezhad, M., Miyashita, Y., Saito, N. and Kokabi, A. H. 2017. Influence of ambient and cryogenic temperature on friction stir processing of severely deformed aluminum

- with SiC nanoparticles. *Journal of Alloys and Compounds*. 718: 361-372. doi: 10.1016/j.jallcom.2017.05.234.
- [14] Fratini, L., Buffa, G. and Shivpuri, R. 2010. Mechanical and metallurgical effects of in process cooling during friction stir welding of AA7075-T6 butt joints. *Acta Materialia*. 58(6): 2056-2067. doi: 10.1016/j.actamat.2009.11.048.
- [15] Fratini, L., Buffa, G. and Shivpuri, R. 2018. Microstructure, mechanical properties and strengthening mechanism of titanium particle reinforced aluminum matrix composites produced by submerged friction stir processing. *Materials Science and Engineering: A*. 734: 353-363. doi: 10.1016/j.msea.2018.08.015.
- [16] Rui-Dong, F., Zeng-Qiang, S., Rui-Cheng, S., Ying, L., Hui-Jie, L. and Lei, L. 2011. Improvement of weld temperature distribution and mechanical properties of 7050 aluminum alloy butt joints by submerged friction stir welding. *Materials & Design*. 32(10): 4825-4831. doi: 10.1016/j.matdes.2011.06.021.
- [17] Sharma, C., Dwivedi, D.K. and Kumar, P. 2012. Influence of in-process cooling on tensile behaviour of friction stir welded joints of AA7039. *Materials Science and Engineering: A*. 556: 479-487. doi: 10.1016/j.msea.2012.07.016.
- [18] Khodabakhshi, F., Gerlich, A. P., Simchi, A. and Kokabi, A. H. 2015. Cryogenic friction-stir processing of ultrafine-grained Al-Mg-TiO₂ nanocomposites. *Materials Science and Engineering: A*. 620: 471-482. doi: 10.1016/j.msea.2014.10.048.
- [19] Ramezani, N. M., Rasti, A., Sadeghi, M. H., Pour, B. J. and Hajideh, M. R. 2016. 2016. Experimental study of tool wear and surface roughness on high speed helical milling in D2 steel. *Modares Mech Eng*. 15(20): 198-202. doi: 10.1001.1.10275940.1394.15.13.72.2.
- [20] Molla Ramezani, Ranjbar, H., Sadeghi, M.H. and Rasti, A. 2016. Helical milling of cold-work AISI D2 steel with PVD carbide tool under dry conditions. *Modares Mechanical Engineering*. 15(13): 203-206. doi: 10.1001.1.10275940.1394.15.13.53.3.
- [21] Molla Ramezani, N., Rezaei Hajideh, M. and Shahmirzaloo, A. 2017. Experimental study of the cutting parameters effect on hole making processes in hardened steel. *Journal of Modern Processes in Manufacturing and Production*. 6(3):67-76. doi: 10.1001.1.27170314.2017.6.3.5.0.
- [22] Ashish, B., Saini, J. and Sharma, B. 2016. A review of tool wear prediction during friction stir welding of aluminium matrix composite. *Transactions of Nonferrous Metals Society of China*. 26(8): 2003-2018. doi: 10.1016/S1003-6326(16)64318-2.
- [23] Molla Ramezani, N., Davoodi, B., Aberoumand, M. and Rezaei Hajideh, M. 2019. Assessment of tool wear and mechanical properties of Al 7075 nanocomposite in friction stir processing (FSP). *Journal of the Brazilian Society of Mechanical Sciences and Engineering*. 41: 1-14. doi: doi.org/10.1007/s40430-019-1683-1.
- [24] Molla Ramezani, N., Davoodi, B., Farahani, M. and Khanli, A. H. 2019. Surface integrity of metal matrix nanocomposite produced by friction stir processing (FSP). *Journal of the Brazilian Society of Mechanical Sciences and Engineering*. 41: 1-11. doi: 10.1007/s40430-019-2014-2.
- [25] Fernandez, G. and Murr, L.E. 2004. Characterization of tool wear and weld optimization in the friction-stir welding of cast aluminum 359+ 20% SiC metal-matrix composite. *Materials Characterization*. 52(1): 65-75. doi: 10.1016/j.jmst.2017.11.029.

- [26] Zhang, H., Wang, D., Xue, P., Wu, L. H., Ni, D. R., Xiao, B. L. and Ma, Z. Y. 2018. Achieving ultra-high strength friction stir welded joints of high nitrogen stainless steel by forced water cooling. *Journal of materials science & technology*. 34(11): 2183-2188. doi: 10.1016/j.jmst.2018.03.014.
- [27] Prado, R. A., Murr, L. E., Soto, K. F. and McClure, J. C. 2003. Self-optimization in tool wear for friction-stir welding of Al 6061+ 20% Al₂O₃ MMC. *Materials science and engineering*: 349(1-2): 156-165. doi: 10.1016/S0921-5093(02)00750-5.
- [28] Nandan, R., Roy, G. G., Lienert, T. J. and Debroy, T. 2007. Three-dimensional heat and material flow during friction stir welding of mild steel. *Acta materialia*. 55(3): 883-895. doi: 10.1016/j.actamat.2006.09.009.
- [29] Khodabakhshi, F. and Gerlich, A. 2018. Potentials and strategies of solid-state additive friction-stir manufacturing technology: A critical review. *Journal of Manufacturing Processes*. 36: p. 77-92. doi: 10.1016/j.jmapro.2018.09.030.
- [30] Nazari, M., Eskandari, H. and Khodabakhshi, F. 2019. Production and characterization of an advanced AA6061-Graphene-TiB₂ hybrid surface nanocomposite by multi-pass friction stir processing. *Surface and Coatings Technology*. 377: 124914. doi: 10.1016/j.surfcoat.2019.124914.
- [31] Zuo, L., Shao, W., Zhang, X. and Zuo, D. 2022. Investigation on tool wear in friction stir welding of SiCp/Al composites. *Wear*. 498: 204331. doi: 10.1016/j.wear.2022.204331.
- [32] Gerlich, A.P. 2017. Critical Assessment 25: Friction stir processing, potential and problems. *Materials Science and Technology*. 33(10):1139-1144. doi: 10.1080/02670836.2017.1300420.
- [33] Zhang, H., Liu, H. and Yu, L. 2011. Microstructure and mechanical properties as a function of rotation speed in underwater friction stir welded aluminum alloy joints. *Materials & Design*. 32(8-9): 4402-4407. doi: 10.1016/j.matdes.2011.03.073.
- [34] Upadhyay, P. and Reynolds, A.P. 2010. Effects of thermal boundary conditions in friction stir welded AA7050-T7 sheets. *Materials Science and Engineering: A*. 527(6): 1537-1543. doi: 10.1016/j.msea.2009.10.039.
- [35] Fatchurrohman, N. and Abdullah, A. 2018. Surface Roughness and Wear Properties of Al–Al₂O₃ Metal Matrix Composites Fabricated Using Friction Stir Processing. *Lecture Notes in Intelligent Manufacturing & Mechatronics (Conference paper)*. doi: 10.1007/978-981-10-8788-2_15.
- [36] Kumar, A., Godasu, A. K., Pal, K. and Mula, S. 2018. Effects of in-process cryocooling on metallurgical and mechanical properties of friction stir processed Al7075 alloy. *Materials Characterization*. 144: 440-447. doi: 10.1016/j.matchar.2018.08.001.
- [37] Yildiz, Y. and Nalbant, M. 2008. A review of cryogenic cooling in machining processes. *International Journal of Machine Tools and Manufacture*. 48(9): 947-964. doi: 10.1016/j.ijmachtools.2008.01.008.
- [38] Hotami, M.M. and Yang, S. 2023. Investigation on Micro-Hardness, Surface Roughness and SEM of Nano TiO₂/B₄C/Graphene Reinforced AA 7075 Composites Fabricated by Frictional Stir Processing. *Crystals*. 13(3): 522. doi: 10.3390/cryst13030522.
- [39] Molla Ramezani, N., Davoodi, B. and Rezaee Hajideh, M. 2018. Investigating the performance of coated carbide insert in hard steel helical milling. *ADMT Journal*. 11(3): 1-9.

- [40] Akbarpour, M. R., Mirabad, H. M., Gazani, F., Khezri, I., Chadegani, A. A., Moeini, A. and Kim, H. S. 2023. An overview of friction stir processing of Cu-SiC composites: microstructural, mechanical, tribological, and electrical properties. 27: 1317-1349. *Journal of Materials Research and Technology*. doi: 10.1016/j.jmrt.2023.09.200.
- [41] Dwivedi, S. P., Sharma, S., Li, C., Zhang, Y., Kumar, A., Singh, R. and Abbas, M. 2023. Effect of nano-TiO₂ particles addition on dissimilar AA2024 and AA2014 based composite developed by friction stir process technique. *Journal of Materials Research and Technology*. 26: 1872-1881. doi: 10.1016/j.jmrt.2023.07.234.
- [42] Hirata, T., Oguri, T., Hagino, H., Tanaka, T., Chung, S. W., Takigawa, Y. and Higashi, K. 2007. Influence of friction stir welding parameters on grain size and formability in 5083 aluminum alloy. *Materials Science and Engineering: A*. 456(1-2): 344-349. doi: 10.1016/j.msea.2006.12.079.
- [43] Imani, H., Molla Ramezani, N., Sadeghi, M. H. and Rasti, A. 2016. The effect of hole making method on cutting force and surface roughness. *Modares Mechanical Engineering*. 15(13): 285-290. doi: 10.1001.1.10275940.1394.15.13.29.9.
- [44] Devaraju, A. and Kishan, V. 2018. Influence of cryogenic cooling (liquid nitrogen) on microstructure and mechanical properties of friction stir welded 2014-T6 aluminum alloy. *Materials Today: Proceedings*, 5(1): 1585-1590. doi: 10.1016/j.matpr.2017.11.250.